Iranian Journal of Numerical Analysis and Optimization
Vol. 14, No. 2, 2024, pp 475–499
https://doi.org/10.22067/ijnao.2024.85218.1335
https://ijnao.um.ac.ir/

Research Article

Drug release from a two-layer stent coating considering the viscoelastic property of the arterial wall: A mathematical and numerical study

E. Azhdari* and A. Emami

Abstract

Atherosclerosis is one of the most common diseases in the world. Medication with metal stents plays an important role in treating this disease. There are many models for delivering drugs from stents to the arterial wall. This paper presents a model that describes drug delivery from the stent coating layers to the arterial wall tissue. This model complements the previous models by considering the mechanical properties of the arterial wall tissue, which changes due to atherosclerosis and improves results

*Corresponding author

Received 6 November 2023; revised 5 February 2024; accepted 28 February 2024

Ebrahim Azhdari
Department of Mathematics, Salman Farsi University of Kazerun, Iran. e-mail: e.azhdari@kazerunsfu.ac.ir

Aram Emami
Department of Mathematics, Salman Farsi University of Kazerun, Iran. e-mail: emami@kazerunsfu.ac.ir

How to cite this article
Azhdari, E. and Emami, A., Drug release from a two-layer stent coating considering the viscoelastic property of the arterial wall: A mathematical and numerical study. *Iran. J. Numer. Anal. Optim.*, 2024; 14(2): 475-499. https://doi.org/10.22067/ijnao.2024.85218.1335

for designing stents. The stability behavior of the model is analyzed, and a number of numerical results are provided with explanations. A comparison between numerical and experimental results, which examine a more accurate match between the in vivo and in vitro, is shown.

AMS subject classifications (2020): 65M06.

Keywords: Stent coating; Viscoelastic; Mathematical model; Numerical simulation.

1 Introduction

Atherosclerosis is a condition in which plaques made up of cholesterol, fat, cellular waste, calcium, and fibrin (a type of insoluble coagulation protein) form inside the arteries and block them [21] (see Figure 1). Methods used to reduce the severity of atherosclerosis include bypass grafting (BG), coronary skin intervention, and less invasive balloon angioplasty [12].

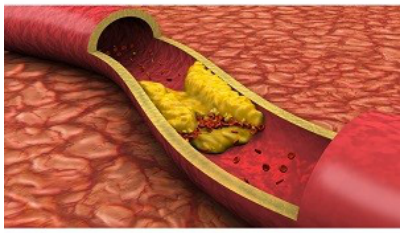

Figure 1: Atherosclerosis. Source: Intermountain Medical Center https://healthcare-in-europe.com/en/news/potential-breakthrough-in-determining-who-s-at-risk.html

Recently, though, a new procedure called stent-based delivery has been introduced that claims to help open blocked vessels and prevent restenosis [3, 28]. The bare metal stent is the first type of stent that is used as a scaffold to prevent restenosis of blood vessels (see Figure 2). Another kind of stent that is used to open blocked vessels and prevent restenosis is a drug-eluting stent [20]. In drug-eluting stents, the drug is gradually removed from the

stent, which makes the drug enter the vessels with sufficient concentration in a timely manner and a biologically active state. This helps keep the arteries smooth and open and allows blood to flow well. Clinical evidence shows that drug effectiveness depends on release rate, drug diffusion rate, drug distribution in tissue, stent design, and so on. Therefore, it is necessary to study the relationship between stent design and the release and retention of eluted drugs.

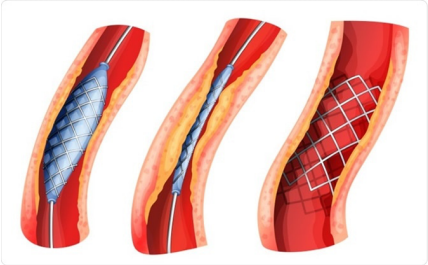

Figure 2: Stent. Source: Image by brgfx on Freepik.com
https://bjbas.springeropen.com/articles/10.1186/s43088-023-00382-9/figures/1

Recently, researchers have studied different types of drug delivery based on stents, including spreading the drug from a metal stent surface as a Dirichlet condition [15, 22], single-layer coating of the drug on the metal wire [11, 16], and also multi-layer coating [14, 24]. For example, Sarifuddin and Mandal [24] have studied the benefits of replacing a single-layer coating with a multi-layer coating along with transfer, which includes better control over drug delivery. Multi-layer coating with different drug forms or release kinetics can provide better control over the drug transfer and treatment process.

Atherosclerosis can affect the thickest arterial layer in advanced stages, and this effect can cause a significant change in the mechanical properties of the arterial wall tissue [10]. All of the above studies have examined drug transfer from stents to arterial wall tissue, regardless of the viscoelastic properties of the arterial wall tissue. The model we present is based on a model presented in [24] and has the potential to help stent designers reduce adverse patient outcomes. The present study aims to investigate more precisely the drug delivery through a two-layer stent coating to the arterial wall tissue taking into account the mechanical properties of the arterial wall tissue. More-

over, the model presented in this paper better agrees with the experimental results than the previous models.

The paper is organized as follows: Section 2 presents a brief clinical perspective of the work. Section 3 describes the model, including the model geometry, a mathematical description of the equations governing drug delivery from the stent coating to the arterial wall tissue, and initial, boundary, and interface boundary conditions. The stability behavior of the model is analyzed in Section 4. Numerical simulations for drug delivery from stent layers to the arterial wall tissue are given in Section 5. Finally, some discussions and conclusions are mentioned in Sections 6 and 7.

2 Clinical perspective

Atherosclerosis is one of the most serious and common cardiovascular diseases in the artery wall. This disease causes blockage of the lumen and reduces blood flow. Surgical techniques, such as coronary artery BG and percutaneous coronary intervention, are techniques used to reduce the severity of advanced atherosclerotic stenosis in the coronary artery. Balloon angioplasty was considered a less invasive intervention to open the blocked lumen. Clinical observations show that balloon angioplasty is associated with restenosis. The advent of bare metal stents has revolutionized balloon angioplasty by reducing the risk of restenosis. However, after several decades of using these types of stents, internal restenosis, that is, re-narrowing of the lumen, was seen again, which was a major defect. Therefore, the drug-eluting stent was invented to overcome the restenosis within the stent after implantation. Atherosclerosis mainly affects the intima, but the periphery, which is the thickest arterial layer, can be affected in advanced stages. This causes a significant change in the mechanical properties of the arterial wall. Several authors have studied mathematical models for drug delivery in cardiovascular tissues. Most of these studies focus on drug diffusion while ignoring the mechanical properties of the arterial wall. In this paper, we study the effect of the mechanical properties of the arterial wall, which has not been considered in the models that are used to deliver drugs from two-layer stents to the arterial wall.

3 Mathematical model

This section describes the mathematical model of the problem, which consists of four parts: geometry of the model (Section 3.1), description of the drug in the stent coating layers (Section 3.2), description of the drug in the arterial wall tissue (Section 3.3), and interface boundary conditions (Section 3.4). The governing equations describe the release of the drug from stent coating layers S_1 (inner layer) and S_2 (outer layer) into the arterial wall tissue V. The parameters used in the model are demonstrated in Table 1 with the relevant descriptions and units.

Table 1: The values used in the model for the parameters.

Variable/Parameter	Description	Value	Reference
$U_{\max}$	maximum velocity (cm/s)	14	[24, 29]
ρ_t	tissue density (g/cm^3)	1.06	[5]
μ_t	viscosity (g/cms)	0.0072	[5]
V_{filt}	filtration velocity (cm/s)	5.8×10^{-6}	[25]
P_k	permeability (cm^2)	2×10^{-14}	[5]
D_t	tissue diffusivity (cm^2/s)	3.65×10^{-8}	[6]
D_1	coating (S_1) diffusivity (cm^2/s)	1×10^{-9}	[6]
D_2	coating (S_2) diffusivity (cm^2/s)	1×10^{-9}	[6]
D_v	viscoelastic diffusion coefficient $(g/(cmsPa))$	5×10^{-11}	Ref. model
B_M	tissue-binding capacity (mM)	1.3	[13]
K_D	constant (mM)	0.136	[13]
D_a	Damkohler number	2700	[27]
r_0	lumen radius (cm)	0.15	[2, 30]
r_1	thickness of coating (S_1) (cm)	0.0025	[24]
r_2	thickness of coating (S_2) (cm)	0.0025	[24]
T	thickness of wall (cm)	0.05	[2, 30]
τ	relaxation time (s)	0.5	Ref. model
τ_σ	relaxation time (s)	0.1	Ref. model
κ	Young modulus (MPa)	0.0001	Ref. model

3.1 Geometry of the model

This section describes the model's geometry using a special stent shape with a half-embedded metal piece and a two-layer coating. To simplify the calculations, a two-dimensional figure has been used instead of a three-dimensional one (see Figure 3). Also, S_1 and S_2 show the inner and outer layers of the stent coating, and V shows the arterial wall tissue. The boundary between lumen and arterial wall tissue is called Γ_l. Γ_w is a boundary between arterial wall tissue and other arterial wall tissue. The boundary between arterial wall tissue and perivascular wall is called Γ_a. Moreover, $\Gamma_{S_1,V}$ is an interface boundary between arterial wall tissue and the inner layer of the stent coating. The interface boundary between the inner and outer layers of the stent coating is called Γ_{S_1,S_2}, and finally, the interface boundary between the outer layer of the stent coating and the metal part of the stent is called Γ_S.

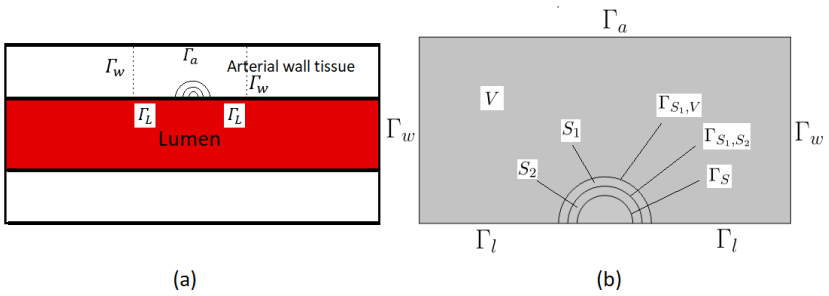

Figure 3: A schematic of the geometric shape of the problem

3.2 Description of the drug in the stent coating layers

In this section, we will study the release of the drug from the stent coating layers. The drug is first loaded solidly into the stent coating. As the stent coating comes into contact with the fluid and the fluid enters the layers through their boundaries, the layer's pores open. The fluid contacts the drug, and the drug begins to release. The drug released along the stent coating layers is described by the following non-dimensionalized equations:

$$\frac{\partial c_m}{\partial t} = -\nabla . J_{c_m} \text{ in } S_m \times (0, T_f], \quad m = 1, 2, \tag{1}$$

where $c_m, m = 1, 2$ are the concentrations of the drug in the stent coating $(S_m, m = 1, 2)$, respectively, $J_{c_m} = -\frac{1}{Pe_m}\nabla c_m$ is the flux of the drug concentration in the stent coating $(S_m, m = 1, 2)$, and T_f is the final time. The parameters $Pe_m, m = 1, 2$ are the Peclet numbers for the coating layers defined by $Pe_m = \frac{R_0 U_0}{D_m}, m = 1, 2$, where $D_m, m = 1, 2$ are the diffusion coefficient of the drug in coating layers $S_m, m = 1, 2$, respectively, and $R_0 = \frac{r_0}{6}$ and $U_0 = \frac{U_{\max}}{6}$ in which r_0 and $U_{\max}$ denote the luminal radius and the maximum velocity at the inlet, respectively.

At time $t = 0$, we assume that the amount of drug released after contacting the loaded drug with the fluid in the stent coating is as follows:

$$c_m(0) = 1, \qquad m = 1, 2. \tag{2}$$

We assume a non-flux boundary condition on the Γ_S, that $J_{c_2}.\eta = 0$ because the drug is impermeable to the metal part of the stent, where η is the exterior unit normal. The drug enters the inner stent coating via boundary conditions from the outer stent coating and then enters the arterial wall tissue through the inner stent coating. Section 3.4 describes the interface boundary conditions.

3.3 Description of the drug in the arterial wall tissue

The equations used to describe the distribution of the drug in the wall are as follows:

Convection is caused by the flow of interstitial fluid within the porous arterial wall, and the continuity equation can be written in dimensionless form in two-dimensional form. The Brinkman equation provides more accurate results because it combines the linear momentum and mass conservation of

fluids in large pores and channels with the Darcy equation for regions with unresolved pores [7]. Therefore, the Brinkman equation is used as follows:

$$\begin{cases} \dfrac{\partial \mathbf{v}}{\partial t} + (\mathbf{v}.\nabla)\mathbf{v} = -\nabla P + \dfrac{1}{Re}\nabla.(\nabla \mathbf{v} + (\nabla \mathbf{v})^T) - \dfrac{1}{ReK_p}\mathbf{v}, \\ \nabla.\mathbf{v} = 0 \quad \text{in} \quad V \times (0, T_f], \end{cases} \tag{3}$$

where $Re = \frac{\rho_t U_0 R_0}{\mu_t}$ and $K_p = \frac{P_k}{R_0^2}$ in which P_k is the Darcy permeability. Here, $\mathbf{v}$ is the velocity vector for the tissue domain, ρ_t is the density, μ_t is the viscosity, and P is the pressure.

To complete the equation (3), the following boundary and initial conditions are given: We assume the initial condition $\mathbf{v}(0) = 0$ and boundary conditions on the boundaries Γ_l, Γ_a and Γ_w (see Figure 3), as follows:

$$\begin{cases} \mathbf{v} = 0 \quad \texttt{on } \Gamma_w, \\ \mathbf{v} = (v_x, v_y) = (0, V_{filt}) \quad \texttt{on } \Gamma_l, \\ P = 0 \quad \texttt{on } \Gamma_a, \end{cases} \tag{4}$$

where V_{filt} is the filtration velocity of plasma.

A drug that does not bind to tissue receptors is known as a free drug, the concentration which is indicated by c_t. Its equation in the arterial wall tissue is as follows:

$$\frac{\partial c_t}{\partial t} = -\nabla.J_{c_t} - \frac{\partial b_t}{\partial t} \quad \text{in} \quad V \times (0, T_f], \tag{5}$$

where $J_{c_t} = -(\frac{1}{Pe_t}\nabla c_t + \frac{1}{D_\sigma}\nabla \sigma - \mathbf{v}c_t)$ is the free drug mass flux, and σ is the response of arterial wall tissue to strain caused by drug molecules. Moreover, Pe_t is the Peclet number for tissue defined by $Pe_t = \frac{R_0 U_0}{D_t}$, where D_t is the diffusion coefficient of the drug in the arterial wall tissue. Also, $D_\sigma = \frac{R_0 U_0}{D_v}$, where D_v is the viscoelastic diffusion coefficient. Finally, b_t is the concentration of a drug that attaches to tissue receptors in the arterial wall and is known as a bound drug, which is described by the following equation:

$$\frac{\partial b_t}{\partial t} = k_a c_t (B_M - b_t) - k_d b_t \quad \text{in} \quad V \times (0, T_f], \tag{6}$$

where $k_a = \frac{K_a R_0}{U_0}$ and $k_d = \frac{K_d R_0}{U_0}$ in which K_a and K_d are the aggregation and disintegration rate constants, respectively, where $K_a = \frac{D_t D_a}{B_M T^2}$ and $K_d = K_a K_D$.

The second sentence of J_{c_t} in equation (5), which is $\frac{1}{D_\sigma}\nabla\sigma$, describes the mechanical behavior of the arterial wall tissue. In other words, it describes the arterial wall as a barrier that prevents the drug from entering the wall. Using the same symbols used in [8] for stress and viscoelastic diffusion coefficient, the model from [4]

$$\sigma + \tau\frac{\partial\sigma}{\partial t} = -\kappa(c_t + \tau_\sigma\frac{\partial c_t}{\partial t}) \quad \text{in} \quad V \times (0, T_f], \tag{7}$$

is similar to the equation used by [19]. Also, κ is the Young modulus, and τ and τ_σ are the relaxation time.

The initial and boundary conditions are taken into account to complete the equations (5) and (7). As in the initial time, there is no free drug and bound drug in the arterial wall, so we have

$$c_t(0) = b_t(0) = 0. \tag{8}$$

Due to the fact that the free drug does not cross the arterial walls ($\Gamma_w \cup \Gamma_a$) as well as the boundary between the lumen and the tissue of the arterial wall (Γ_l), there is a boundary condition $J_{c_t}.\eta = 0$ on the boundaries $\Gamma_l \cup \Gamma_w \cup \Gamma_a$.

3.4 Interface boundary conditions

Aside from the initial and boundary conditions, Systems (1), (3), (5), and (7) are completed by the interface boundary conditions between the first and second layers of the stent coating (Γ_{S_1,S_2}) and the second layer of the stent coating and the arterial wall ($\Gamma_{S_1,V}$) as follows:

$$\begin{cases} J_{c_1}.\eta = -A_2 c_2 \ \texttt{on}\ \Gamma_{S_1,S_2}, \\ J_{c_1}.\eta = -J_{c_2}.\nu \ \texttt{on}\ \Gamma_{S_1,S_2}, \\ J_{c_1}.\eta = A_1 c_1 \ \texttt{on}\ \Gamma_{S_1,V}, \\ J_{c_1}.\eta = -J_{c_t}.\nu \ \texttt{on}\ \Gamma_{S_1,V}, \end{cases} \tag{9}$$

where A_1 and A_2 are partition coefficients.

4 Energy estimates

In this section, we obtain an upper bound for the energy estimate, which is defined as follows:

$$\mathcal{E}(c(t)) = \|c(t)\|^2 + \int_0^t \|\nabla c(s)\|^2 ds + \int_0^t \|c(s)\|^2_{(\Gamma_{S_1,S_2}\cup\Gamma_{S_1,V})} ds,$$

where $c(t) = (c_1(t), c_2(t), c_t(t))$ and $\|\cdot\|$ represent the usual norm in $L^2(\Omega)$ $\big(\Omega = S_1 \cup S_2 \cup V\big)$, which is induced by the corresponding inner product $(\cdot,\cdot)$ [1]. After solving (7), we get the following equation:

$$\sigma = \frac{\kappa}{\tau}(\frac{\tau_\sigma}{\tau} - 1)\int_0^t e^{\frac{1}{\tau}(s-t)} c_t(s) ds + \frac{\kappa\tau_\sigma}{\tau} e^{\frac{-t}{\tau}} c_t(0) - \frac{\kappa\tau_\sigma}{\tau} c_t + e^{\frac{-t}{\tau}}\sigma(0). \quad (10)$$

Replacing (6) in (5) to get

$$\frac{\partial c_t}{\partial t} = \nabla.(\frac{1}{Pe_t}\nabla c_t + \frac{1}{D_\sigma}\nabla\sigma - \mathbf{v}c_t) - k_a c_t(B_M - b_t) + k_d b_t. \quad (11)$$

The weak formulation of the differential problem (1) and (11) is defined as follows: Find $c(t) \in H^1(S_1) \times H^1(S_2) \times H^1(V)$ such that $\frac{\partial c}{\partial t}(t) \in L^2(S_1) \times L^2(S_2) \times L^2(V)$, $c(0) = (1, 1, 0)$, and

$$\begin{aligned}(\frac{\partial c}{\partial t}(t), u) = \sum_{i=1,2,t} (-\frac{1}{Pe_i}\nabla c_i, \nabla u_i) + (A_2c_2, u_1)_{\Gamma_{S_1,S_2}} - (A_1c_1, u_1)_{\Gamma_{S_1,V}} \\ -(A_2c_2, u_2)_{\Gamma_{S_1,S_2}} - ((\frac{1}{D_\sigma}\nabla\sigma - \mathbf{v}c_t), \nabla u_t) + (A_1c_1, u_t)_{\Gamma_{S_1,V}} \\ -(k_a c_t(B_M - b_t), u_t) + (k_d b_t, u_t), \end{aligned} \quad (12)$$

where $(u_1, u_2, u_t) \in (H^1(S_1) \times H^1(S_2) \times H^1(V))$.

Replacing (10) in (12) by considering $\sigma(0)$ and $c_t(0)$ as a constant to get

$$\begin{aligned}(\frac{\partial c}{\partial t}(t), u) = \sum_{i=1,2,t} (-\frac{1}{Pe_i}\nabla c_i, \nabla u_i) + (A_2c_2, u_1)_{\Gamma_{S_1,S_2}} - (A_1c_1, u_1)_{\Gamma_{S_1,V}} \\ -(A_2c_2, u_2)_{\Gamma_{S_1,S_2}} + \frac{\kappa}{D_\sigma\tau}(1 - \frac{\tau_\sigma}{\tau})\int_0^t e^{\frac{1}{\tau}(s-t)}(\nabla c_t(s), \nabla u_t(s)) ds \\ +\frac{\kappa\tau_\sigma}{D_\sigma\tau}(\nabla c_t, \nabla u_t) + (\mathbf{v}c_t, \nabla u_t) + (A_1c_1, u_t)_{\Gamma_{S_1,V}} \\ -(k_a c_t(B_M - b_t), u_t) + (k_d b_t, u_t). \end{aligned} \quad (13)$$

Theorem 1. If $c(t) = (c_1(t), c_2(t), c_t(t))$ is a solution to the variational problem (13), then

$$\mathcal{E}(c(t)) \leq \frac{1}{\phi_{\min}} \mathcal{E}(c(0)) e^{\phi t}, \tag{14}$$

where $\phi = \frac{\phi_{\max}}{\phi_{\min}}$ is a time independent positive constant, with $\phi_{\min} = \min\{1, \frac{2}{Pe_1}, \frac{2}{Pe_2}, 2(\frac{1}{Pe_t} - \frac{\kappa\tau_\sigma}{D_\sigma\tau} - \epsilon_2^2), +2A_1, 2A_2\}$ and

$$\begin{aligned}\phi_{\max} = \max\{&(\frac{1}{2\epsilon_2^2}\|\mathbf{v}\|^2_{L^\infty(L^\infty)} - 2k_aB_M + 2k_a\delta\|b_t\|_{L^\infty(L^\infty)}), 2\epsilon_1^2A_2, \frac{A_2}{2\epsilon_1^2},\\ &2\frac{\kappa}{D_\sigma\tau}(1 - \frac{\tau_\sigma}{\tau}), 2\epsilon_3^2A_1, \frac{A_1}{2\epsilon_3^2}\},\end{aligned}$$

where $\epsilon_1, \epsilon_2, \epsilon_3 \neq 0$ are positive constants and $\left(\frac{1}{Pe_t} - \frac{\kappa\tau_\sigma}{D_\sigma\tau} - \epsilon_2^2\right) > 0$.

Proof. In (13), replace u_1, u_2, and u_t with c_1, c_2 and c_t, respectively, to get

$$\begin{aligned}\frac{1}{2}\frac{\partial}{\partial t}\|c(t)\|^2 = &-\frac{1}{Pe_i}\sum_{i=1,2,t}\|\nabla c_i\|^2 + (A_2c_2, c_1)_{\Gamma_{S_1,S_2}} - A_1\|c_1\|^2_{\Gamma_{S_1,V}}\\ &-A_2\|c_2\|^2_{\Gamma_{S_1,S_2}} + \frac{\kappa}{D_\sigma\tau}(1 - \frac{\tau_\sigma}{\tau})\int_0^t e^{\frac{1}{\tau}(s-t)}\|\nabla c_t(s)\|^2 ds\\ &+\frac{\kappa\tau_\sigma}{D_\sigma\tau}\|\nabla c_t\|^2 + (\mathbf{v}c_t, \nabla c_t) + (A_1c_1, c_t)_{\Gamma_{S_1,V}}\\ &-(k_ac_t(B_M - b_t), c_t) + (k_db_t, c_t).\end{aligned} \tag{15}$$

Using the Cauchy–Schwarz inequality and since $k_d = K_Dk_a$ assuming $\delta > 1$ such that $c_t \geq \frac{K_D}{\delta - 1}$

$$\begin{aligned}\frac{1}{2}\frac{\partial}{\partial t}\|c(t)\|^2 \leq &\sum_{i=1,2,t} -\frac{1}{Pe_i}\|\nabla c_i\|^2 + \epsilon_1^2A_2\|c_2\|^2_{\Gamma_{S_1,S_2}} + \frac{A_2}{4\epsilon_1^2}\|c_1\|^2_{\Gamma_{S_1,S_2}}\\ &-A_1\|c_1\|^2_{\Gamma_{S_1,V}} - A_2\|c_2\|^2_{\Gamma_{S_1,S_2}}\\ &+\frac{\kappa}{D_\sigma\tau}(1 - \frac{\tau_\sigma}{\tau})\int_0^t e^{\frac{1}{\tau}(s-t)}\|\nabla c_t(s)\|^2 ds + \frac{\kappa\tau_\sigma}{D_\sigma\tau}\|\nabla c_t\|^2\\ &+\epsilon_2^2\|\nabla c_t\|^2 + \frac{1}{4\epsilon_2^2}\|\mathbf{v}\|^2_{L^\infty(L^\infty)}\|c_t\|^2 + \epsilon_3^2A_1\|c_1\|^2_{\Gamma_{S_1,V}}\\ &+\frac{A_1}{4\epsilon_3^2}\|c_t\|^2_{\Gamma_{S_1,V}} - k_aB_M\|c_t\|^2 + k_a\delta\|b_t\|_{L^\infty(L^\infty)}\|c_t\|^2.\end{aligned}$$

Let $\epsilon_2 > 0$ such that $\left(\frac{1}{Pe_t} - \frac{\kappa\tau_\sigma}{D_\sigma\tau} - \epsilon_2^2\right) > 0$ and $\left(\frac{1}{4\epsilon_2^2}\|\mathbf{v}\|^2_{L^\infty(L^\infty)} - k_aB_M + k_a\delta\|b_t\|_{L^\infty(L^\infty)}\right) > 0$. Then

$$\frac{1}{2}\frac{\partial}{\partial t}\|c(t)\|^2+\sum_{i=1,2}\frac{1}{Pe_i}\quad\|\nabla c_i\|^2+\big(\frac{1}{Pe_t}-\frac{\kappa\tau_\sigma}{D_\sigma\tau}-\epsilon_2^2\big)\|\nabla c_t\|^2+A_1\|c_1\|^2_{\Gamma_{S_1,V}}$$
$$+A_2\|c_2\|^2_{\Gamma_{S_1,S_2}}\le\big(\frac{1}{4\epsilon_2^2}\|\mathbf{v}\|^2_{L^\infty(L^\infty)}-k_aB_M+k_a\delta\|b_t\|_{L^\infty(L^\infty)}\big)\|c_t\|^2$$
$$+\epsilon_1^2A_2\|c_2\|^2_{\Gamma_{S_1,S_2}}+\frac{A_2}{4\epsilon_1^2}\|c_1\|^2_{\Gamma_{S_1,S_2}}$$
$$+\frac{\kappa}{D_\sigma\tau}(1-\frac{\tau_\sigma}{\tau})\int_0^t e^{\frac{1}{\tau}(s-t)}\|\nabla c_t(s)\|^2ds$$
$$+\epsilon_3^2A_1\|c_1\|^2_{\Gamma_{S_1,V}}+\frac{A_1}{4\epsilon_3^2}\|c_t\|^2_{\Gamma_{S_1,V}}.\qquad(16)$$

Multiplying (16) by two and taking integration to get

$$\mathcal{E}(c(t))\le\frac{1}{\phi_{\min}}\mathcal{E}(c(0))+\phi\int_0^t\mathcal{E}(c(s))ds,$$

using the Gronwall lemma [9] to obtain (14).

□

The estimation we obtained in Theorem 1 allows us to determine the uniqueness of the solution (13) and its stability for a limited time.

5 Numerical simulations

COMSOL 5.3 Multiphysics is utilized for meshing and numerical results. The arterial wall and coating layers are meshed, as shown in Figure 4. The following modules in the COMSOL are used:

- Brinkman equations in order to calculate the velocity and pressure of the arterial wall;
- Coefficient form partial differential equation (c) in order to calculate the drug concentration in the coating layers and arterial wall tissue.

To make sure that the numerical results do not depend on the mesh size, we consider the following meshes:

- Mesh 1: 1642 elements;

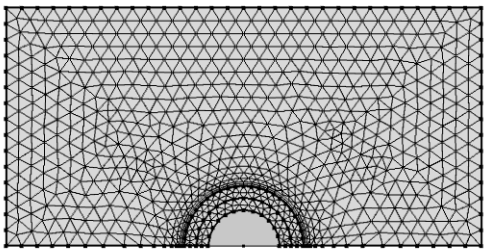

Figure 4: Computational meshes in the domain

Table 2: Different errors for free drug concentration in arterial wall.

h	L^∞	L^2	H^1
0.001	1.3×10^{-12}	1.54×10^{-11}	3.81×10^{-10}
0.01	2.2×10^{-12}	2.14×10^{-11}	5.88×10^{-10}
0.1	3.6×10^{-12}	3.56×10^{-11}	7.43×10^{-10}

- Mesh 2: 3132 elements;
- Mesh 3: 6162 elements;
- Mesh 4: 12340 elements.

The adequacy of the mesh density has been investigated using convergence tests. By considering two different meshes, the solutions' convergence and the mesh's independence have been investigated. To illustrate this claim more clearly, Figure 5 and Table 2 show the comparison among different meshes for the average drug concentration in arterial wall tissue. Of note, the reference solution is defined by $h_{\max} = 1 \times 10^{-4}$. According to this figure, the changes among the meshes are almost unrecognizable, suggesting that the numerical results do not depend on the mesh size.

Based on Figure 6, the velocity vectors affect both the distribution and retention of the drug. This result indicates the boundary condition for the

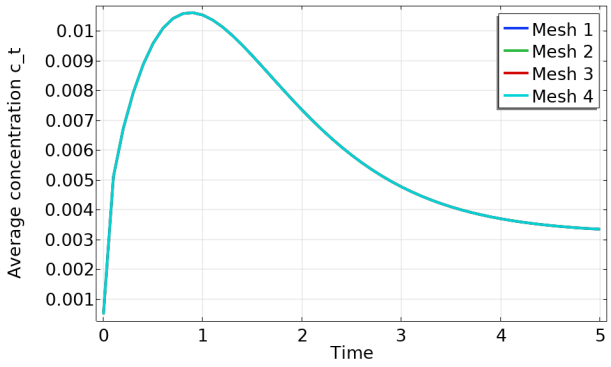

Figure 5: Average drug concentration (c_t) in the arterial wall.

interface boundary between the lumen and the arterial wall tissue. The velocity vector is indicated by an arrow. These results are consistent with the results in [28].

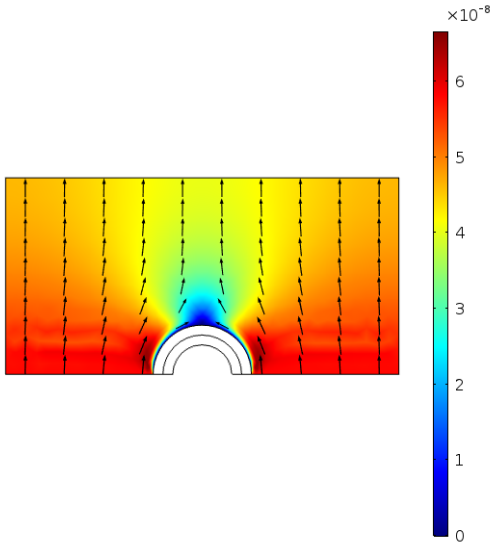

Figure 6: Dissemination of the velocity vector

The filtration velocity used in [24], which is derived from experimental results performed on animals [25], is similar to the amounts obtained in [17, 23, 30]. Figure 7 shows the low effect of filtration velocity on the average

drug concentration in arterial wall tissue for $1.8 \times 10^{-6}(cm/s)$ and $5.8 \times 10^{-6}(cm/s)$.

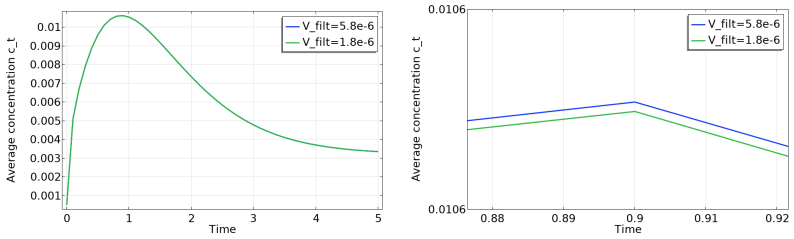

(a) (b) zoom of (a) around t=0.9

Figure 7: The effect of filtration velocity (V_{filt}) on the average drug concentration c_t in the arterial wall tissue.

The release of drug concentration from the stent coating layers into the arterial wall tissue during 300 seconds has been demonstrated in Figure 8. As shown in Figure 8, the drug concentration enters from the inner layer of the stent coating due to the interface boundary condition on $\Gamma_{S_1,V}$. Over time, the drug concentration enters from the inner layer of the stent coating and increases in the arterial wall tissue.

The local concentration of the free and bound drug, which is indicated by a red point (see Figure 9 (f)), is illustrated in Figure 9. According to these figures, the concentration of free drug increases for a certain period of time and then diminishes (Figure 9 (a) and (c)), although the bound drug goes up to reach a steady state (Figure 9 (b) and (d)). By comparing the rate of drug release from the inner and outer layers of the stent, it can be seen that a faster release leads to a higher concentration of the free and bounded drug in the arterial wall. For further explanation, we need to point out that the rapid diffusion in the inner layer compared to the outer layer has a higher concentration in the arterial wall tissue, which is around 0.16 in the inner layer (Figure 9 (a)) and around 0.12 in the outer layer (Figure 9 (c)). This is because the inner layer is closer to the arterial wall. Moreover, Figure 9 (e) shows the role of convective flow in drug delivery to (at the reference point) the arterial wall tissue. It is clear that convection contributes significantly to

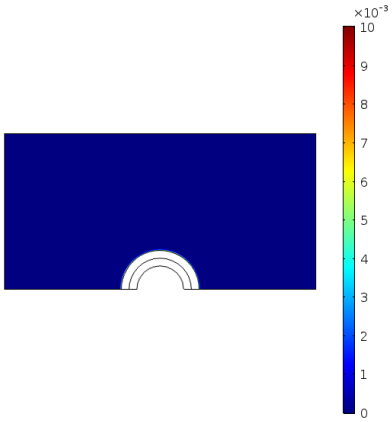

(a) Drug release, 0 second

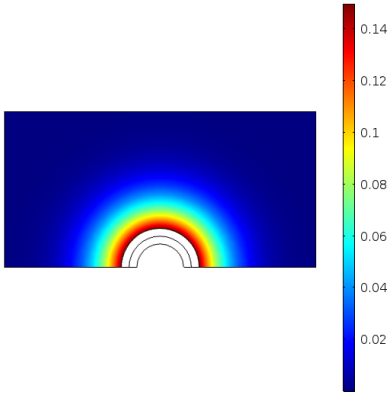

(b) Drug release, 25 second

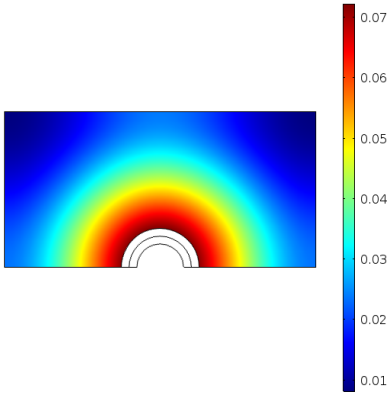

(c) Drug release, 100 second

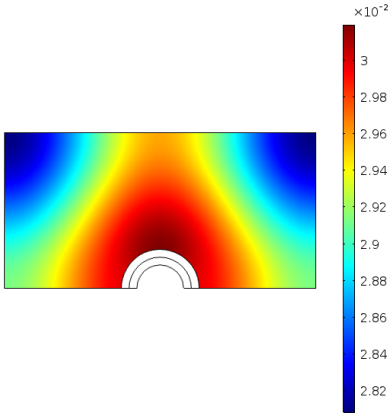

(d) Drug release, 300 second

Figure 8: Dissemination for different times

drug delivery, which must be taken into account in order to achieve better results.

The behavior of mean drug concentration in the inner and outer layers of the stent for different diffusion coefficients is shown in Figure 10. This figure shows that the reduction of the diffusion coefficient in the inner and outer layers of the stent makes the drug enter the arterial wall tissue with a delay from the stent. This enables the stent designers to deliver the required amount of drug to the arterial wall tissue.

The average free drug in arterial wall tissue is depicted in Figure 11. This figure shows that the drug concentration tends to increase from zero to maximum and diminishes afterward. It is interesting to note that in the case of fast release of the inner layer ($D_1 = 1 \times 10^{-9} cm^2/s$) and slow release of the outer layer ($D_2 = 1 \times 10^{-11} cm^2/s$), this maximum is higher than in the case of slow release of the inner layer ($D_1 = 1 \times 10^{-11} cm^2/s$) and slow release of the outer layer ($D_2 = 1 \times 10^{-11} cm^2/s$).

The arterial wall tissue has a viscoelastic property, which significantly affects drug delivery. As a result, we presented this effect in Figure 12. It can be seen that the higher the viscoelastic diffusion coefficient, D_v, the less drug is observed in the arterial wall tissue. In other words, the tissue of the arterial wall has a barrier property against drug delivery.

In order to validate the application of the model presented in this paper, in Figure 13, we compare the numerical results obtained for the free drug concentration in the arterial wall with the in-vivo experimental data (Sarifuddin and Mandal [24], Tzafriri et al. [26], and Mongrain et al. [18]). It is clear that considering the viscoelastic properties of the arterial wall can affect the transfer of free drugs from the stent coating layers to the arterial wall. These results indicate that the proposed model is congruent with the models proposed in Sarifuddin,Tzafriri,Mongrain, although they did not take into account the viscoelastic properties of the arterial wall. In other words, the model presented in this paper is more consistent with the experimental results than other models since the viscoelastic property, which is one of the mechanical properties of the arterial wall tissue that acts as a barrier, has been considered. Figure 13 illustrates the advantages of this article compared to the previous ones.

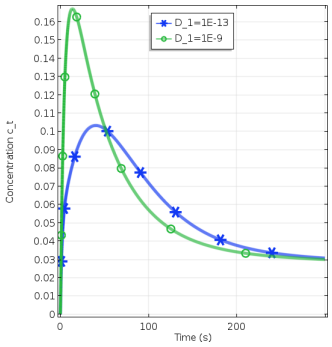

(a) The effect of D_1 on the free drug

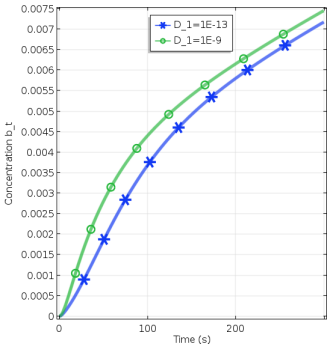

(b) The effect of D_1 on the bound drug

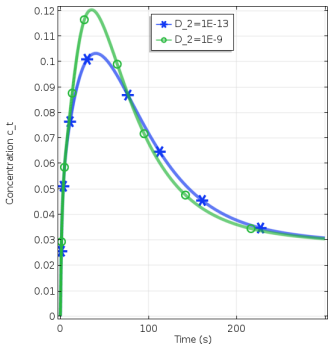

(c) The effect of D_2 on the free drug

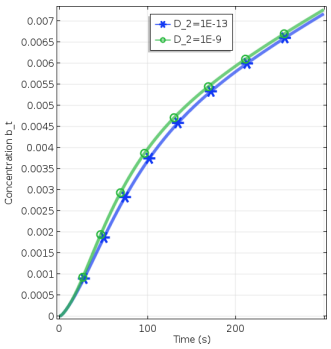

(d) The effect of D_2 on the bound drug

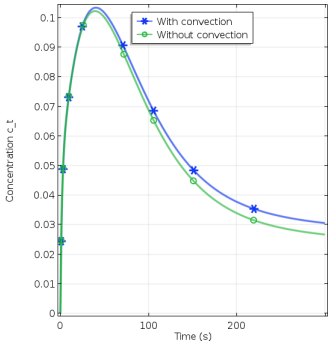

(e) The role of convection on the free drug

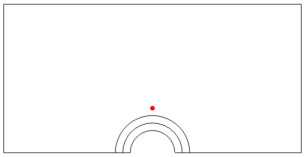

(f) reference point

Figure 9: The effect of the diffusion coefficient of the layers of stent coating on free and bound drug concentration and the effect of convection on free drug concentration in the arterial wall tissue.

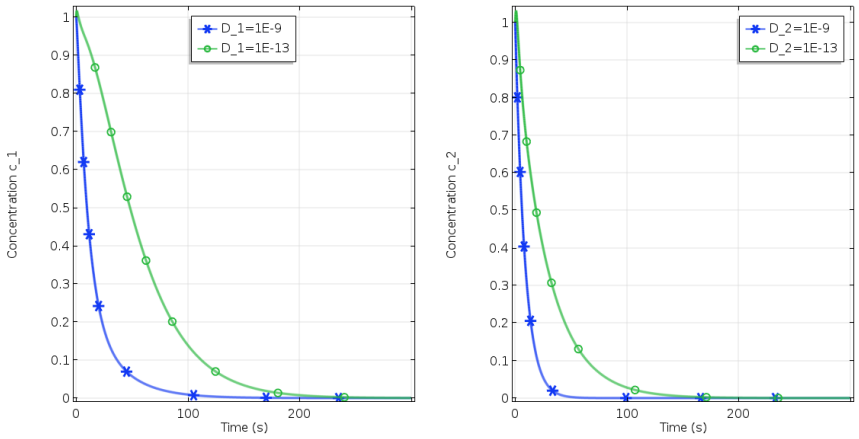

(a) inner layer, S_1 (b) outer layer, S_2

Figure 10: The effect of diffusion coefficients on the drug in coating layers

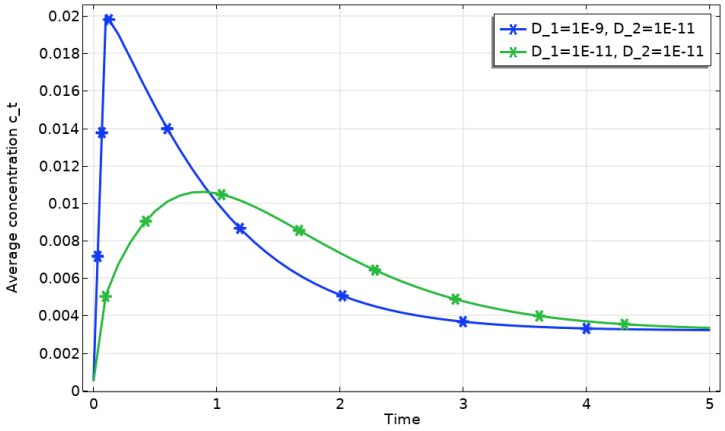

Figure 11: The average concentration of free drug in arterial wall tissue (the effect of diffusion coefficients on drug in coating layers)

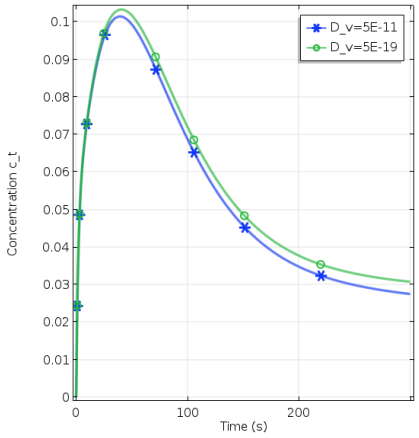

Figure 12: The influence of D_v on the concentration of free drug in arterial wall tissue

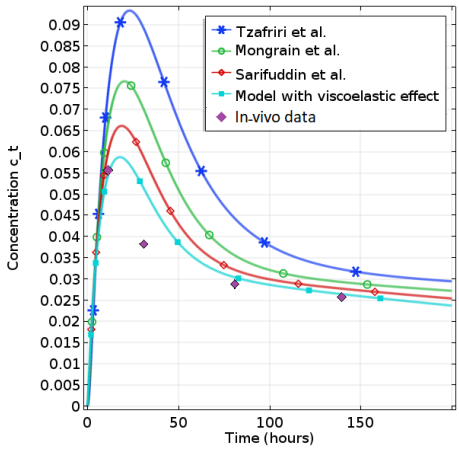

Figure 13: Comparison between experimental data and the model presented for drug delivery from stent coating layers into the arterial wall

6 Discussion

In order to discuss the transfer of drugs from a half-embedded two-layer coating stent into arterial walls with viscoelastic properties, the following points can be specified. In Figure 5, the independence of numerical results from the mesh size is discussed. The effect of the velocity vectors on the distribution and retention of the drug is shown in Figure 6, which corroborates the results in [28]. The effect of filtration velocity on the average drug concentration in arterial wall tissue is shown in Figure 7. An increase in time indicates a rise in the concentration of the drug in the tissue of the arterial wall, which can be seen in Figure 8. As Figure 9 demonstrates, the concentration of the bound drug increased and reached a steady state, while the concentration of the free drug went up for some time but then decreased. In addition, faster release results in higher concentrations of free and bound drugs in the arterial wall. Because the inner layer is closer to the arterial wall, the rapid diffusion of the inner layer is greater than the concentration of the outer layer in the arterial wall tissue. Additionally, convection significantly contributes to drug delivery. Figure 10 shows that the reduction of the diffusion coefficient in the inner and outer layers of the stent makes the drug enter the arterial wall tissue with a delay, which allows the stent designers to determine the amount of drugs required for the arterial wall tissue. When the inner layer is faster than the outer layer, compared with slow release in both layers, the maximum drug concentration is higher, which is observed in Figure 11. Figure 12 illustrates that the viscoelastic property of arterial wall tissue acts as a barrier against drug transmission, which is not discussed in similar works. Finally, a comparison between the experimental data and the proposed model for drug delivery from the stent coating layers to the arterial wall, which exhibits greater agreement than other models, is presented in Figure 13.

7 Conclusion

Considering the mechanical properties of the arterial wall due to atherosclerotic changes provided a deeper understanding of the stent's performance. It

enabled a better agreement between the mathematical model and the experimental results. A mathematical model is presented to consider the transport of drugs from the stent layers to the arterial wall and describes the convective flow due to the flow of interstitial fluid in the arterial wall tissue as well as the viscoelastic property of the arterial wall. Presenting an upper bound for the energy estimate determines the uniqueness of the solution and its stability for a limited time. Finally, the numerical simulation verifies the agreement between the mathematical model, numerical results, and experimental results.

Acknowledgments

The authors would like to express their profound gratitude to the editor and anonymous reviewers for their remarkable dedication and invaluable feedback, which greatly enhanced the quality of the paper.

References

[1] Azhdari, E. and Naghipoor, J. *The effect of viscoelasticity of the tissue on the magneto-responsive drug delivery system*, J. Math. Biol. 84 (13) (2022) 1–26.

[2] Baroldi, G., Bigi, R. and Cortigiani, L. *Ultrasound imaging versus morphopathology in cardiovascular diseases. Coronary atherosclerotic plaque*, Cardiovasc Ultrasound 2(1) (2004) 1–10.

[3] Bozsak, F., Chomaz, J-M. and Barakat, A.I. *Modeling the transport of drugs eluted from stents: physical phenomena driving drug distribution in the arterial wall*, Biomech. Model. Mechanobiol.13 (2014) 327–347.

[4] Brinson, H.F. and Brinson, L.C. '*Mechanical bioeffects of ultrasound-Polymer Engineering Science and Viscoelasticity: An Introduction*, New York: Springer .2010

[5] Chung, S. and Vafai, K. *Low-density lipoprotein transport within a multilayered arterial wall-effect of the atherosclerotic plaque/stenosis*, J. Biomech. 46 (3) (2013) 574–585.

[6] Creel, C.J., Lovich, M.A. and Edelman, E.R. *Arterial paclitaxel distribution and deposition*, Circ. Res.86 (8) (2000) 879–884.

[7] de Paulo Ferreira, L., de Oliveira, T.D.S., Surmas, R., da Silva, M.A.P. and Peçanha, R.P. *Brinkman equation in reactive flow: Contribution of each term in carbonate acidification simulations*, Adv. Water Resour. 144 (2020) 103696.

[8] Ferreira, J.A., Grassi, M., Gudino, E. and De Oliveira, P. *A new look to non-Fickian diffusion*, Appl. Math. Model. 39 (1) (2015) 194–204.

[9] Gronwall, T.H. *Note on the derivative with respect to a parameter of the solutions of a system of differential equations*, Ann. Math. 20 (1919) 292–296.

[10] Holzapfel, G.A., Gasser, T.C. and Ogden, R.W. *A new constitutive framework for arterial wall mechanics and a comparative study of material models*, J. Elast. 61 (2000) 1–48.

[11] Hossainy, S. and Prabhu, S. *A mathematical model for predicting drug release from a biodurable drug-eluting stent coating,* J. Biomed. Mater. Res A. 87 (2) (2008) 487–493.

[12] Huang, Y., Ng, H.C.A., Ng, X.W. and Subbu, V., *Drug-eluting biostable and erodible stents,* J. Control. Release.193 (2014) 188–201.

[13] Kolachalama, V.B., Pacetti, S.D., Franses, J.W., Stankus, J.J., Zhao, H.Q., Shazly, T., Nikanorov, A., Schwartz, L.B., Tzafriri, A.R. and Edelman, E.R. *Mechanisms of tissue uptake and retention in zotarolimus-coated balloon therapy*, Circulation. 127 (20) (2013) 2047–2055.

[14] McGinty, S., King, D. and Pontrelli, G. *Mathematical modelling of variable porosity coatings for controlled drug release*, Med. Eng. Phys. 45 (2017) 51–60.

[15] McGinty, S., McKee, S., McCormick, C. and Wheel, M. *Release mechanism and parameter estimation in drugeluting stent systems: analytical solutions of drug release and tissue transport,* Math. Med. Biol. 32 (2) (2015) 163–186.

[16] McKittrick, C.M., McKee, S., Kennedy, S., Oldroyd, K., Wheel, M., Pontrelli, G., Dixon, S., McGinty, S. and McCormick, C. *Combining mathematical modelling with in vitro experiments to predict in vivo drug-eluting stent performance*, J. Control. Release.303 (2019) 151–161.

[17] Meyer, G., Merval, R.G. and Tedgui, A. *Effects of pressure-induced stretch and convection on low-density lipoprotein and albumin uptake in the rabbit aortic wall*, Circ. Res. 79 (1996) 532–540.

[18] Mongrain, R., Faik, I., Leask, R.L., Rodés-Cabau, J., Larose, E. and Bertrand, O.F. *Effects of diffusion coefficients and struts apposition using numerical simulations for drug eluting coronary stents*, J. Biomech. Eng. 129 (5) (2007) 733–742.

[19] Naghipoor, J., Ferreira, J.A., de Oliveira, P. and Rabczuk, T. *Tuning polymeric and drug properties in a drug eluting stent: A numerical study*, Appl. Math. Model. 40 (17-18) (2016) 8067–8086.

[20] Nishimoto, Y., Ueda, Y., Sugihara, R., Murakami, A., Ueno, K., Takeda, Y., Hirata, A., Kashiwase, K., Higuchi, Y. and Yasumura, Y., *Comparison of angioscopic findings among secondgeneration drug-eluting stents,* J. Cardiol. 70 (2017) 297–302.

[21] Pericevic, I., Lally, C., Toner, D. and Kelly, D.J. *The influence of plaque composition on underlying arterial wall stress during stent expansion: The case for lesion-specific stents*, Med. Eng. Phys. 31(4), (2009) 428–433.

[22] Pontrelli, G. and De Monte, F. *A multi-layer porous wall model for coronary drug-eluting stents,* Int. J. Heat. Mass. Trans. 53 (2010) 3629–3637.

[23] Prosi, M., Zunino, P., Perktold, K. and Quarteroni, A. *Mathematical and numerical models for transfer of low-density lipoproteins through the arterial walls: a new methodology for the model set up with applications to the study of disturbed lumenal flow,* J. Biomech. 38 (4) (2005) 903–917.

[24] Sarifuddin, Roy, S. and Mandal, P.K. *Computational model of stent-based delivery from a half-embedded two-layered coating*, Comput. Methods. Biomech. Biomed. Engin. 23 (12) (2020) 815–831.

[25] Tedgui, A. and Lever, M. *Filtration through damaged and undamaged rabbit thoracic aorta*, Am. J. Physiol. 247 (5) (1984) H784–H791.

[26] Tzafriri, A.R., Groothuis, A., Price, G.S. and Edelman, E.R. *Stent elution rate determines drug deposition and receptor-mediated effects*, J. Control. Release. 161 (2012) 918–926.

[27] Tzafriri, A.R., Levin, A.D. and Edelman, E.R. *Diffusion limited binding explains binary dose response for local arterial and tumour drug delivery*, Cell Prolif.42(3) (2009) 348–363.

[28] Vairo, G., Cioffi, M., Cottone, R., Dubini, G. and Migliavacca, F. *Drug release from coronary eluting stents: a multidomain approach,* J. Biomech. 43(8) (2010) 1580–1589.

[29] Welkowitz, W. *Engineering hemodynamics: application to cardiac assist devices*, J. Clin. Eng. 13, no. 2 (1988) 79.

[30] Yang, N. and Vafai, K. *Modeling of low-density lipoprotein (LDL) transport in the artery effects of hypertension*, Int. J. Heat. Mass. Transf. 49 (5-6) (2006) 850–867.